THE JOURNAL OF PHYSICAL CHEMISTRY C

Article

pubs.acs.org/JPCC

Multicomponent Gas Storage in Organic Cage Molecules

Fei Zhang,[†] Yadong He,[†] Jingsong Huang,[‡] Bobby G. Sumpter,[‡] and Rui Qiao*[,†]

[†]Department of Mechanical Engineering, Virginia Tech, Blacksburg, Virginia 24061, United States

[‡]Center for Nanophase Materials Sciences and Computational Sciences & Engineering Division, Oak Ridge National Laboratory, Bethel Valley Road, Oak Ridge, Tennessee 37831, United States

Supporting Information

ABSTRACT: Porous liquids are a promising new class of materials featuring nanoscale cavity units dispersed in liquids that are suitable for applications such as gas storage and separation. In this work, we use molecular dynamics simulations to examine the multicomponent gas storage in a porous liquid consisting of crown-ether-substituted cage molecules dissolved in a 15-crown-5 solvent. We compute the storage of three prototypical small molecules including CO_2, CH_4, and N_2 and their binary mixtures in individual cage molecules. For porous liquids in equilibrium with a binary 1:1 gas mixture bath with partial gas pressure of 27.5 bar, a cage molecule shows a selectivity of 4.3 and 13.1 for the CO_2/CH_4 and CO_2/N_2 pairs, respectively. We provide a molecular perspective of how gas molecules are stored in the cage molecule and how the storage of one type of gas molecule is affected by other types of gas molecules. Our results clarify the molecular mechanisms behind the selectivity of such cage molecules toward different gases.

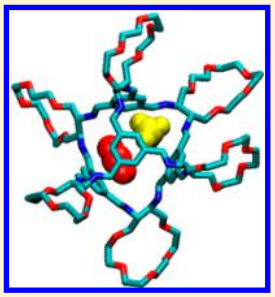

1. INTRODUCTION

New types of porous materials, ranging from zeolites to metal−organic frameworks (MOFs),[1,2] have been continuously proposed and synthesized over the past few decades. Owing to their high porosity and large surface area, these materials have found applications in a broad range of fields such as molecular separation, energy storage, and heterogeneous catalysis.[3−5] However, these porous materials including zeolites and MOFs mainly exist as solids, making it more difficult to implement them in a typical flow process than liquids. Because of the challenges toward practical applications posed by the solid nature of these materials, especially at large scales, developing liquid state porous materials has been actively pursued in the past.[6−14] In this regard, the synthesis of organic cage-like molecules in 2009[9] is a critical step toward developing such materials[15−17] since it has been considered by some experts in the community as introducing "a new branch in the evolutionary tree of porous materials" beyond zeolites and MOFs.[18] Such cage molecules provide a porous unit that can be dissolved into liquids without breaking any chemical bonds. Since then, rapid progress has been made toward making porous liquids using organic cage molecules.[10−12,19,20] While the initial attempts made by attaching long hydrocarbon chains to the organic cage-like molecules led to a lower melting point, the porosity was easily destroyed in liquid state due to the penetration of hydrocarbon chains into the cage cavities.[12] Most recently, with ingenuity in chemical design and aid of computational tools, Giri and colleagues successfully prepared and characterized the first organic molecular porous liquids.[13] Specifically, they coupled crown ether functionalized diamines with 1,3,5-triformylbenzenes and dissolved the resultant cage molecules at high concentration into a 15-crown-5 solvent. They also reported a porous liquid system with scrambled cage molecules dissolved in hexachloropropene solvents.[13] These porous liquids thus prepared are potentially effective gas absorbents, which can be transported and implemented relatively easily in industrial systems.

The currently available porous liquids have already shown promise in some areas including gas storage and separation.[18] Nevertheless, as with many other revolutionary and novel materials, the best applications of porous liquids may not have been identified, and the development of porous liquids for intended applications is still at an early stage. Despite this, it is safe to expect that the adsorption of small molecules inside the organic cage molecules will play a critical role in most, if not all, applications of porous liquids. Therefore, there is a great need to develop a fundamental understanding for the adsorption of gas molecules in the organic cage molecules dispersed in liquid solvents.[21] Molecular dynamics (MD) simulations can be a powerful tool for this purpose; e.g., MD has been used to show that solvent molecules in the porous liquids synthesized recently must pay a very high free energy cost to enter the organic cage, and thus the intrinsic cavity of the organic cage molecules is maintained in the porous liquids.[13,22] We previously studied the thermodynamics as well as kinetics for the storage of pure CO_2, CH_4, and N_2 molecules in crown-ether-substituted cage molecules dissolved in a 15-crown-5 solvent using MD simulations.[23] We showed that the storage capacity of gas in a cage molecule is governed by the nonelectrostatic (dispersive) intermolecular interactions between the gas and the cage and by the size/shape of the gas molecules. The gas molecules considered can enter the cage molecule without a notable barrier and exit the cage on a nanosecond time scale.

Received: February 8, 2017
Revised: May 17, 2017
Published: May 18, 2017

DOI: 10.1021/acs.jpcc.7b01260
J. Phys. Chem. C 2017, 121, 12426−12433

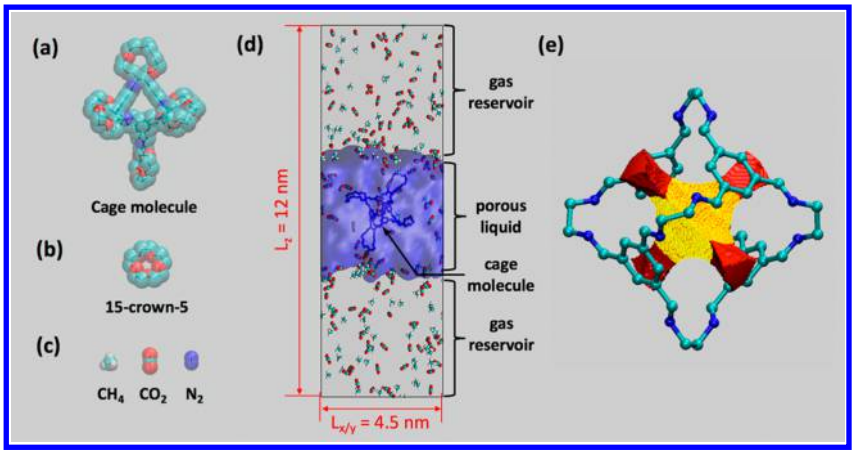

Figure 1. Molecular modeling of gas storage in porous liquids. (a–c) Molecular models of the crown-ether-substituted cage molecule (a), the solvent molecule (b), and the gas molecules (c). (d) A snapshot of the simulation system consisting of porous liquids (rendered as isosurface in blue) in equilibrium with a binary mixture of CO_2 and CH_4. (e) Volume rendering of the accessible space in a cage molecule superimposed on the molecular model of the cage. The accessible space is probed using an atom of 0.28 nm in diameter. The accessible space within a radial distance of 0.28 nm from the cage center is shown in yellow; the accessible space within a radial distance of 0.28–0.5 nm from the cage center is shown in red. For clarity, the hydrogen atoms of the cage molecule and the solvent molecule are not shown. In (e), crown ether tails are not shown.

In this work, we study the adsorption of prototypical small gas molecules including CO_2, CH_4, and N_2 in porous liquids that are in equilibrium with gas-phase reservoirs containing either pure gas or binary mixtures of different gases. We seek to understand how the presence of multiple gas species affects the adsorption of gas molecules inside individual cage molecules, in particular, how different gas molecules compete with each other for adsorption inside a cage molecule and how a cage molecule accommodates more than one molecule inside it. The former aspect is relevant to the application of porous liquids for gas adsorption and separation. The latter aspect is potentially relevant to applications in which the organic cage molecules in the porous liquids are used as a medium for confining small molecules to study their fundamental properties or as a nanoscale reactor. The rest of the article is organized as follows. Section 2 describes the simulation system and methods. Section 3 presents the results for storage of pure gas and binary mixture in individual cage molecules and the underlying molecular mechanisms. Finally, conclusions are drawn in section 4.

2. SIMULATION SYSTEM AND METHODS

We use MD simulations to study the storage of gas molecules in the organic cage molecules dissolved in molecular solvents. Figure 1a–c shows the molecular structures of the cage molecule, the 15-crown-5 solvent molecule, and the CO_2, CH_4, and N_2 gas molecules. The crown-ether-substituted cage molecule (porous unit) consists of an organic cage-like octahedron and six looped crown ether tails (see Figure 1a). The cage-like octahedron provides a nonspherical cavity and four access windows allowing gas molecules to get in/out of the cage cavity. Because both the crown ether tails of the cage molecules and the solvent molecules (Figure 1b) have a circular structure that limits their access to the cage's cavity, the liquid mixture of the cage molecules and the solvents together form a porous liquid. The gas molecules considered here (see Figure 1c) are relatively small and thus can be stored inside the cage molecule. These gas molecules differ in both shape and size: the CH_4 molecule, although explicitly modeled by one C atom and four H atoms as a tetrahedron shape, has a rather spherical shape with an effective diameter of 0.42 nm,[24,25] while CO_2 and N_2 molecules are both rod-like. The long and short axes of the CO_2 molecule (0.52 and 0.34 nm, respectively) are slightly longer than those of the N_2 molecule (0.41 and 0.30 nm, respectively).[26] As shown below, the shape and size of gas molecules play an important role in determining their storage capacity inside the cage molecules and the selectivity of cage molecules toward different gas molecules.

Figure 1d shows a snapshot of the MD system used for the simulations. The system consists of a gas bath (the lower gas reservoir and upper gas reservoir are connected because of the periodic boundary condition) and a slab of porous liquids positioned in the middle of the fully periodic simulation box. The porous liquid is made by dissolving one crown-ether-substituted cage molecule into 170 solvent molecules. Since gas molecules can exchange freely between the liquid phase and gas phase, this setup allows us to study the gas storage under well-controlled partial pressure in the gas phase.

Ideally, a systematic study of the gas storage calls for the computation of the gas adsorption isotherm in the cage molecule by systematically varying the partial pressure of different gas species in the gas bath. However, given the very large parameter space that must be explored in such studies, we focused on two sets of studies in this work. In the first set of study, five systems with identical porous liquid but different gas bath compositions (pure CO_2, pure CH_4, pure N_2, CO_2 + CH_4 mixture, and CO_2 + N_2 mixture) were set up. For these systems, we examined the gas storage under a fixed partial gas pressure in the gas bath instead of computing the gas adsorption isotherm under many different partial pressures. Specifically, the partial pressure of each gas in the gas bath was controlled to be the same in all simulation systems (P_b = 27.5 ± 0.3 bar; see Figure S1 in the Supporting Information). For example, the pressure of CO_2 in the gas bath for the pure CO_2 simulation is the same as the partial pressure of CO_2 in the gas bath for the CO_2 + CH_4 simulation. With a relatively high partial gas pressure to help improve the gas storage statistics inside individual cage molecule, this first set of simulations allows us to gain useful insight into the gas storage by delineating how gas molecules are stored inside a cage and by comparing the results for different gas molecules. In the second set of study, we computed the adsorption isotherm of CO_2 and CH_4 molecules in the cage molecule in equilibrium with the gas

DOI: 10.1021/acs.jpcc.7b01260
J. Phys. Chem. C 2017, 121, 12426–12433

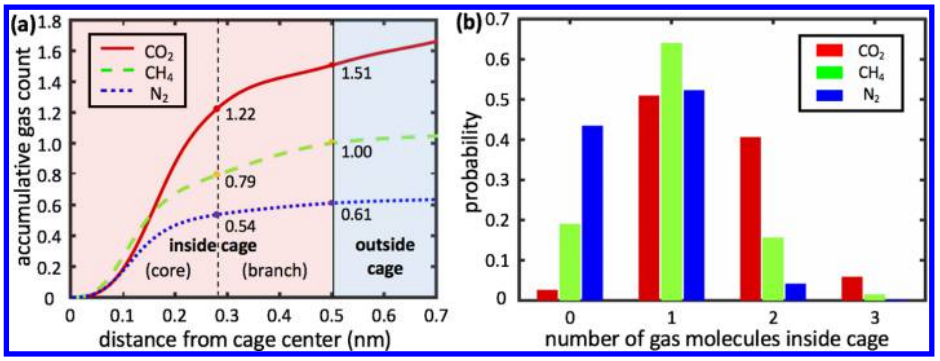

Figure 2. Gas storage in cage molecules dispersed in porous liquids exposed to a gas bath containing pure CO_2, CH_4, and N_2 with a pressure of 27.5 bar. (a) Accumulative gas molecule count as a function of the radial distance from the cage center. The vertical dashed line indicates the boundary between the core and branch regions of the cavity, and the vertical solid line indicates the cage molecule's accessible space. (b) Probability distribution of the number of gas molecules inside a cage. The probability that four or more gas molecules occupy a single cage is <0.1% and thus not shown. The position of gas molecule is based on its center-of-mass.

bath containing CO_2 + CH_4 mixture. To this end, five systems with identical porous liquids but different gas baths were studied. The partial pressures of the CO_2 and CH_4 in the gas bath were equal and varied from 9 to 54 bar in different simulations. This set of simulations allows us to examine the effect of partial pressure on the gas storage inside the cage molecule.

The force fields for all molecules were the same as those adopted in our previous work.[23] Briefly, the cage molecule and the solvent molecule were modeled using the OPLS-AA force fields.[27] The CO_2, CH_4, and N_2 molecules were modeled using the EPM2, OPLS-AA, and TraPPE force fields, respectively.[27−29] The force fields for the cage molecule used here is a reasonable choice because they are compatible with the force fields for the solvent and gas molecules. It has been established that the force fields we adopted for the gas molecules can reproduce their thermodynamic properties such as compressibility and phase diagram quite well and meanwhile are widely used in studying their adsorption behavior in other porous materials such as MOFs.[30] As shown in the first molecular modeling of porous liquids[13] as well as our previous work,[23] these force fields allow the key properties of the solvents, e.g., their density and solubility, to be predicted quite well. In addition, rapid exchange of gas inside and outside the cage molecule was observed in all simulations, which indicates that the gas molecules studied here can enter without notable energy barrier and leave the cage cavity easily, consistent with recent experimental results.[22]

The MD simulations were performed in the NVT ensemble (T = 400 K) using the Gromacs code.[31] Here we adopt a rather high temperature to facilitate both the diffusion of gas molecules in the solvent and the exchange of gas molecules inside and outside the cage molecule. This strategy is often used in the literature, e.g., in the study by Giri et al. MD simulations were performed at 350 and 400 K,[13] and it helps ensure effective sampling of the phase space. The system's temperature was maintained using the V-rescale thermostat with a time constant of 0.1 ps. Electrostatic interactions were computed using the PME method with a real-space cutoff length of 1.4 nm and an FFT spacing of 0.12 nm. The neighbor list was updated every time step. The Lennard-Jones interactions were computed using direct summation with a cutoff at 1.4 nm. All bonds involving hydrogen atoms were constrained using the LINCS algorithm.[32] A time step of 1 fs was used. The center-of-mass motion for system was removed every 0.1 ps to avoid the drift of the porous liquids in the simulation box.

The cage molecule and solvent molecules were first packed into the middle section of the system using the Packmol code.[33] For each system studied, after equilibrating the porous liquids for 5 ns, gas molecules were inserted into the vacuum space at the two sides of the porous liquid. This was followed by another 5 ns equilibration run for the gas molecules to reach equilibrium with the liquid phase. After that, a 40 ns production run was performed. The trajectory of the system was saved every 1 ps for analysis (a video showing a sample trajectory of the CH_4 + CO_2 system can be found in the Supporting Information). To ensure that the gas partial pressure inside the gas bath matches the desired pressure within 2% deviation, we had to iteratively tune the number of gas molecules inside the *entire* system. To obtain reliable statistics, systems in which the partial pressure of gas species in the gas bath is lower than 20 bar were simulated 50 times with independent initial configurations; other systems were simulated 25 times with different initial configurations.

3. RESULTS AND DISCUSSION

Cage Molecule's Accessible Space. We first examine the cavity space inside the cage molecule. The functional part of a cage molecule spans a radius of ∼0.8 nm from its geometrical center. However, because of the steric exclusion by the cage's atoms, the accessible space for gas molecules within a cage molecule is limited to a radial distance of ≤0.5 nm from its geometrical center.[23] Figure 1e shows the volume rendering of this accessible space obtained by probing the cage's interior using an atom with a diameter of 0.28 nm, which roughly corresponds to the short axis of a N_2 molecule. We observe that inside a cage molecule the space available for gas storage consists of a nonspherical central cavity and four corridors connecting its interior to the outside solvents. Following our prior work,[23] we divided the accessible space within a cage molecule into a core region within 0.28 nm from the cage's center (marked by yellow color in Figure 1e) and a branch region spanning a radial distance of 0.28−0.5 nm from the cage's center (marked by red color in Figure 1e).

Storage of Pure Gas Molecules. Next we examine the storage capacity per cage molecule (CPC) when the porous liquids are in equilibrium with pure gas bath with a pressure of 27.5 bar. CPC is defined by the total accumulative count of gas molecules within the cage molecule's accessible space of 0.5 nm

DOI: 10.1021/acs.jpcc.7b01260
J. Phys. Chem. C 2017, 121, 12426−12433

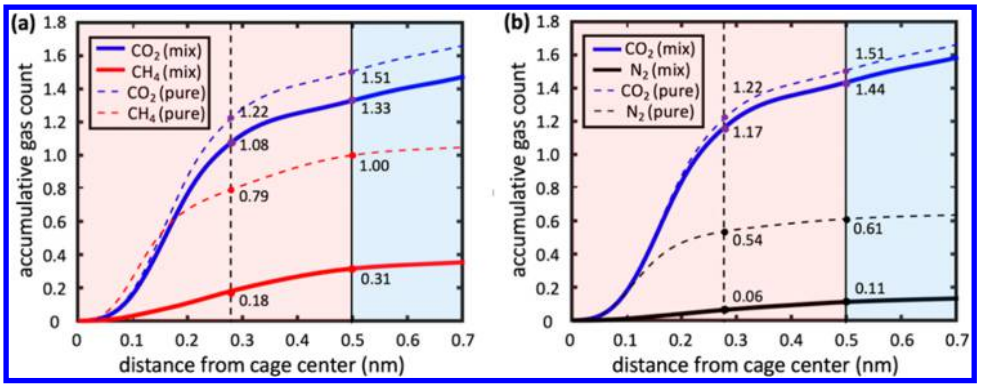

Figure 3. Accumulative gas molecule count as a function of radial distance from the center of the cage molecule in equilibrium with a gas bath containing a mixture of CO_2 and CH_4 molecules (a) and a mixture of CO_2 and N_2 molecules (b). Results for a gas bath containing pure CO_2, CH_4, and N_2 gas are shown using thin dashed curves. The vertical dashed line indicates the boundary between the core and branch regions of the cavity, and the vertical solid line indicates the cage molecule's accessible space. The partial pressure of all gas molecules in the gas bath is 27.5 ± 0.3 bar.

from its center. Figure 2a shows the accumulative count of gas molecules as a function of the distance from the cage center. The contribution from the core region toward CPC is found to be 1.22 ± 0.02, 0.79 ± 0.05, and 0.54 ± 0.06 for pure CO_2, CH_4, and N_2, respectively, while the corresponding contribution from the branch region is found to be 0.29 ± 0.01, 0.21 ± 0.02, and 0.07 ± 0.02. The net CPC is 1.51 ± 0.04, 1.0 ± 0.07, and 0.61 ± 0.07 for CO_2, CH_4, and N_2, respectively. The core region contributes greatly to the overall CPC while the contribution of the branch region is modest and depends on the gas stored. Specifically, for CO_2, CH_4, and N_2, the amount stored in the branch region is ∼24%, 27%, and 13% of that stored in the core region, respectively.

As revealed in our earlier studies, the contribution of cage's core region toward CPC is controlled primarily by the nonelectrostatic gas−cage interactions for gas stored there.[23] The potential energy of a gas molecule stored in the core region due to its van der Waals interactions with the cage was found to be −22.2, −17.3, and −13.3 kJ/mol for CO_2, CH_4, and N_2, respectively. Hence, gas molecules are energetically favored in the core region in the order of CO_2 > CH_4 > N_2, in agreement with their core region's contribution. The contribution of the cage's branch region toward CPC is controlled by both the energetics of gas−cage interactions and entropic effects. For a gas molecule residing in the branch region, its potential energy due to interactions with the cage was found to be −19.5, −14.8, and −10.8 kJ/mol for CO_2, CH_4, and N_2, respectively. While the CO_2−cage interaction energy is still the most negative, CO_2 molecules in the branch region also experience the largest entropic penalty, which disfavors its storage in the branch region. The latter effect is caused by the fact that CO_2 molecules are longer than CH_4 and N_2 molecules, and thus their rotation is hindered the most in the branch region.

In addition to the location that gas molecules are stored inside a cage molecule, we also examined whether, and how, multiple gas molecules coexist inside a cage molecule. The histogram in Figure 2b shows the probabilities of 0, 1, 2, and 3 pure gas molecules being stored in a single cage. For all three gases, the probability that only one gas molecule is stored in a cage is the highest among all scenarios, while the probability that three (or more) gas molecules reside in the same cage is very low. However, for CO_2, the cage is rarely empty (probability: 2.6%), and two molecules often reside in the same cage (probability: 40.6%). In contrast, for N_2, the cage is often empty (probability: 43.4%) and rarely filled with two molecules (probability: 4.1%). The situation for CH_4 lies in between N_2 and CO_2.

We note that the order of the cage's CPC for the molecules computed here (CPC_{CO_2} > CPC_{CH_4} > CPC_{N_2}) differs from that reported in our prior study (CPC_{CH_4} > CPC_{CO_2} > CPC_{N_2}).[23] The difference originates from the different system setups. In our previous work, there was no gas bath and the number of gas molecules in the porous liquids was the same for different gases. Therefore, the gas storage capacity of cage molecules computed from such a setup was affected by the partition of gas molecules between the cage molecule and solvents, and the result is appropriate for closed systems. For open system in which porous liquids are in contact with gas streams, the storage capacity of cage molecules computed in the present study is more practical.

Storage of Multicomponent Gas Molecules. For multicomponent gas storage, we start by examining gas adsorption inside the cage molecule when its host porous liquids are exposed to a 1:1 mixture of CO_2 and CH_4. Here the partial pressure of both gas components in the gas bath is 27.5 bar. Figure 3a shows the accumulative counts of CO_2 and CH_4 molecules in the cage molecule. From these data, the CPC of CO_2 molecule is obtained as 1.33 ± 0.03, which is only 12% lower than the situation when the gas bath is filled with pure CO_2 with the same partial pressure. In comparison, the CPC of CH_4 molecule is significantly reduced to 0.31 ± 0.04, i.e., 69% lower than that for pure CH_4. Therefore, the cage molecule exhibits a high selectivity toward these two molecules. To quantify this selectivity, for a cage in equilibrium with a gas bath containing a mixture of gas molecules A and B, we introduce a selectivity coefficient $S_{A/B}$ for the cage molecule as

$$S_{A/B} = \left(\frac{CPC_A}{CPC_B}\right) \Big/ \left(\frac{p_A}{p_B}\right) \quad (1)$$

where p_A and p_B are the partial pressure of molecules A and B in the gas bath. It follows that the cage molecule studied here gives a selectivity coefficient of S_{CO_2/CH_4} = 4.3. It should be noted that this S_{CO_2/CH_4} is specific to the partial pressure of the two gases studied. However, given that the research on the selectivity of cage molecules for different gas molecules is at a very early stage at present, we defer the systematic investigation

DOI: 10.1021/acs.jpcc.7b01260
J. Phys. Chem. C 2017, 121, 12426−12433

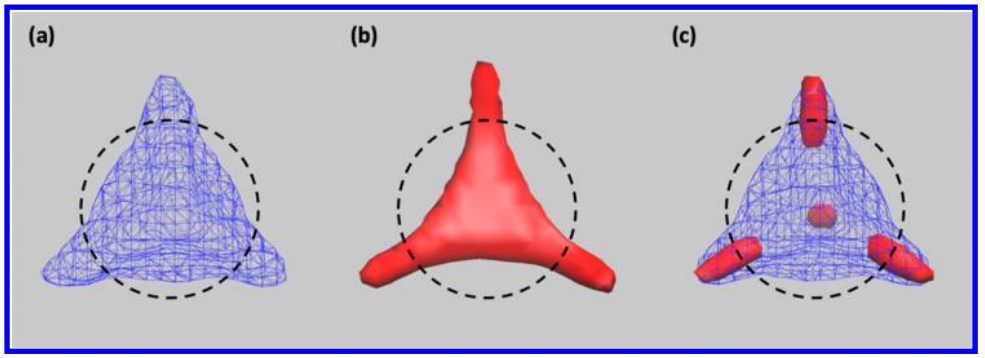

Figure 4. Isosurface of CO_2 (blue) and CH_4 (red) gas density inside a cage molecule in equilibrium with a gas bath containing pure CO_2 (a), pure CH_4 (b), and a mixture of CO_2 and CH_4 molecules (c). The isosurface is set to a density of 15 nm^{-3}. The black dashed circle marks the boundary between the cage's core region and branch regions. The partial pressure of all gas molecules in the gas bath is 27.5 ± 0.3 bar.

of how S_{CO_2/CH_4} varies with the partial pressure of molecules in the gas bath to future studies.

To understand what contributes to the different storage capacity of the cage for the CO_2 and CH_4, we analyze the density isosurface of these molecules inside the cage. Figure 4 shows the results when the cage is in equilibrium with gas baths containing pure CO_2, pure CH_4, and a mixture of CO_2 and CH_4. The isosurface is set to a density value of 15 nm^{-3}, which is high enough so that the isosurface highlights the region where gas molecules are concentrated. We observe that the high density zone of CO_2 molecules inside the cage changes little when we move from the adsorption of pure CO_2 to CO_2 + CH_4 mixtures. However, when we move from adsorption of pure CH_4 to CO_2 + CH_4 mixtures, the high density zone of CH_4 in the cage's core region disappears and the high density zone in the cage's branch region shrinks marginally. Therefore, when CO_2 and CH_4 are both present, there is little effect on the adsorption of CO_2 molecules in the cage. The competition from CO_2 molecules drives CH_4 molecules out of the cage's core region but hardly affects the CH_4 adsorption in the cage's branch region. Overall, the cage molecule's selectivity of CO_2 over CH_4 is mostly contributed by the depletion of CH_4 by CO_2 from the cage's core region.

Next we examine whether, and how, a cage molecule can accommodate more than one molecule. This will not only help understand the gas storage capacity of a cage but also help delineate the state of the gas molecules confined inside the cage. Table 1 shows the probability of finding different numbers of CO_2 and CH_4 molecules inside one cage molecule in equilibrium with a gas bath containing a 1:1 CO_2 + CH_4 mixture. With the gas partial pressure adopted here, while a cage molecule most likely accommodates one CO_2 molecule (probability ∼ 38%), it also frequently hosts two or more gas molecules (probability ∼ 54%). In particular, the probabilities of finding two CO_2 molecules or one CO_2 molecule and one CH_4 molecule inside a cage are ∼29% and ∼14%, respectively. To clarify where these molecules are stored inside the cage when double occupancy occurs, we computed their distribution inside the cage as a function of distance from the cage center. As can be seen from the results shown in Figure 5a, when two CO_2 molecules reside inside the cage, both molecules favor the cage's core region. On the other hand, when two CH_4 molecules reside in a cage, one of them prefers its core region while the other one prefers its branch region (Figure 5b). When one CO_2 molecule and one CH_4 molecule reside in a cage, the CO_2 molecule occupies predominately the core region while the CH_4 molecule is found both in core and branch regions (Figure 5c). These results are consistent with the accumulated gas count data shown in Figure 3a.

Table 1. Probability (in %) of Finding Different Numbers of Gas Molecules inside a Cage in Equilibrium with a Gas Bath Containing a Mixture of CO_2 + CH_4 (P_{CO_2} = P_{CH_4} = 27.5 bar)[a]

		N(CH_4)[c]			
		0	1	2	≥3
N(CO_2)[b]	0	1.5	6.3	1.4	x
	1	38.0	13.6	1.5	x
	2	28.5	4.8	x	x
	3	3.8	x	x	x
	≥4	x	x	x	x

[a]"x" means the probability is less than 0.5%. [b]Number of CO_2 molecules in the cage. [c]Number of CH_4 molecules in the cage.

Overall, when a porous liquid is exposed to a mixture of CO_2 and CH_4 gases, CO_2 molecules adsorb more readily into its cage molecules than the CH_4 molecules, often with two or more CO_2 molecules residing in each cage's core region. Displaced by these CO_2 molecules, the adsorption of CH_4 molecules in the core region is greatly reduced while that in the branch is reduced modestly. Hence, the contribution of the core region and branch region to the storage of CH_4 molecules in a cage is comparable, which differs greatly from the adsorption of pure CH_4. The high occupancy of CO_2 in the core region and its ability to displace CH_4 from this region can be understood as follows. In the core region, a CO_2 molecule's potential energy due to its interaction with the cage (−22.2 kJ/mol) is considerably more negative than that for a CH_4 molecule (−17.3 kJ/mol). This helps multiple CO_2 molecules to be packed into the core region and effectively displace CH_4 molecules. In the branch region, CO_2 molecules only marginally displace the CH_4 molecules because, although CO_2 molecules are again energetically more favored than CH_4 in this region, they suffer larger entropic penalty because their rotation is restricted in the narrow branch region.[23]

The above discussion suggests that the selectivity of the cage toward different gas molecules is controlled primarily by the gas−cage interaction energies of different gases molecules and to a lesser extent by the entropic penalty of different molecules in the branch region. While the cage exhibits a modest selectivity for CO_2 over CH_4, we expect that a stronger selectivity can be achieved if the CH_4 molecule is replaced by a

DOI: 10.1021/acs.jpcc.7b01260
J. Phys. Chem. C 2017, 121, 12426−12433

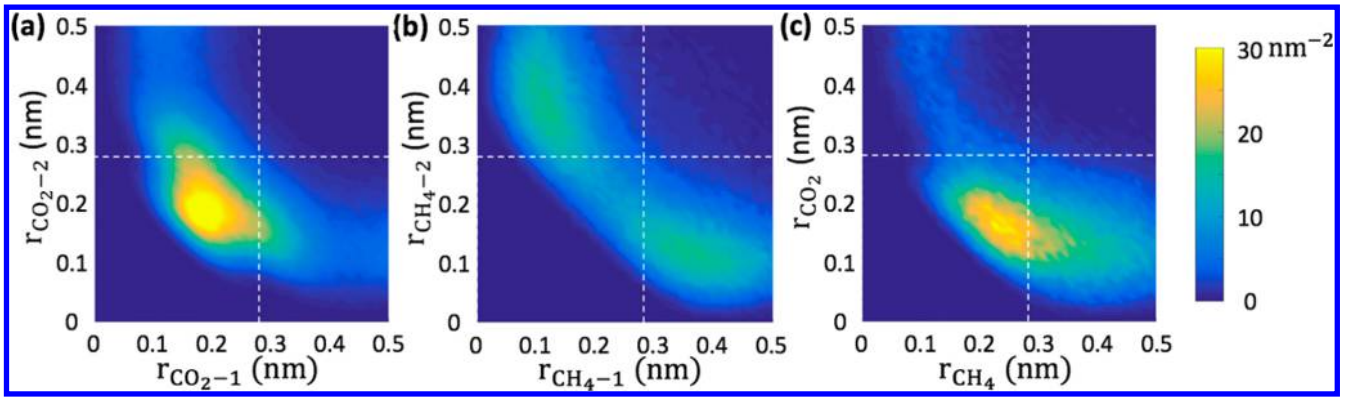

Figure 5. Probability density of the radial distribution of gas molecules inside a cage in equilibrium with a gas bath containing a mixture of CO_2 and CH_4 ($P_{CO_2} = P_{CH_4} = 27.5$ bar). (a) When two CO_2 molecules reside in the cage. (b) When two CH_4 molecules reside in the cage. (c) When one CO_2 molecule and one CH_4 molecule reside in the cage. The axis labels r_A and r_B denote the radial position of molecule A and B inside the cage. The white dashed lines denote the boundary between the core and branch regions inside the cage.

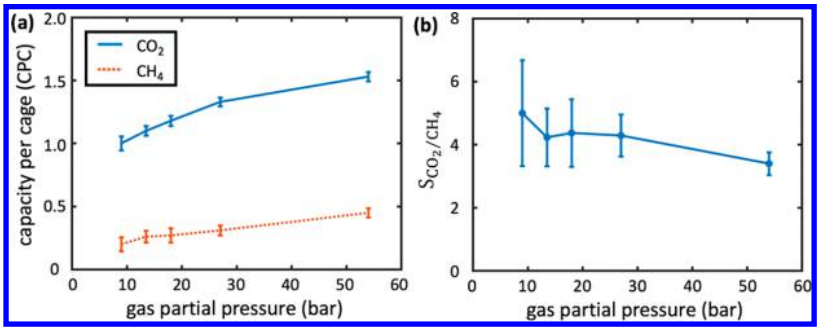

Figure 6. (a) Adsorption isotherm of CO_2 and CH_4 molecules in an organic cage molecule in equilibrium with a gas bath containing 1:1 CO_2 + CH_4 mixture. (b) Selectivity of the cage molecule for the CO_2/CH_4 pair.

molecule that interacts more weakly with the cage and experiences more entropy penalty in the branch region than the CH_4 molecules. The former conditions are satisfied by N_2 molecules. Figure 3b shows the accumulative counts of the CO_2 and N_2 molecules in a cage molecule in equilibrium with a gas bath in which the partial pressure of both CO_2 and N_2 are 27.5 bar. From these data, the CPCs of CO_2 and N_2 molecule are obtained as 1.44 ± 0.05 and 0.11 ± 0.05, respectively, which gives a selectivity of $S_{CO_2/N_2} = 13.1$. This very high selectivity is caused mainly by two factors. First, N_2 molecules are almost fully displaced from the core region by the CO_2 molecules (see Figure 3b and Figure S2 in the Supporting Information). Second, the adsorption of N_2 molecules in the branch region is low even without the competition from CO_2 molecules (see Figure 2a).

Thus far, we focused on the gas storage inside cage molecules in equilibrium with gas baths with a specific partial gas pressure. It is also essential to know how the selectivity of the cage varies with partial gas pressure. Using the second set of simulations described in section 2, we computed the adsorption isotherm of the cage molecule in equilibrium with a gas bath containing 1:1 CO_2 + CH_4 mixture (i.e., $P_{CO_2} = P_{CH_4}$). Figure 6a shows the CPCs of CO_2 and CH_4 at different partial gas pressures. Over the range of partial pressures explored, CO_2 is always more competitive than CH_4 in adsorbing in the cage, which is consistent with our observation made at a gas partial pressure of 27.5 bar. Figure 6b shows the selectivity of the cage molecule for the CO_2/CH_4 pair. At partial pressure of 9−27.5 bar, the variation of the cage's selectivity of CO_2 over CH_4 is within the statistical uncertainty. However, as the partial pressure increases to 54 bar, the selectivity of CO_2 over CH_4 decreases slightly, which we attribute to the entropic effect. Specifically, as the partial pressure increases, the cage becomes packed with more gas molecules, which imposes an entropic penalty for gas adsorption inside the cage. Such an entropic penalty is more significant for the bulkier CO_2 molecules than for the CH_4 molecule. We note that a similar mechanism has been used to explain why the bulkier C_2H_6 molecules become less competitive in adsorbing in zeolites compared to the smaller CH_4 molecules.[34,35]

4. CONCLUSIONS

In summary, we have examined the storage of three prototypical small molecules (CO_2, CH_4, and N_2) and their binary mixtures within organic cage molecules using MD simulations. In all cases, the cage was in equilibrium with a gas bath, and the partial pressure of each type of molecule in the gas bath was kept the same. For a partial pressure of 27.5 bar, a cage molecule gives a selectivity of 4.3 and 13.1 for the CO_2 + CH_4 and CO_2 + N_2 pairs, respectively. The selectivity of CO_2 over CH_4 and N_2 is attributed to its stronger van der Waals interactions with the cage, which helps CO_2 molecules displace CH_4/N_2 molecules from the cage's core region. Nevertheless, CO_2 molecules do not effectively displace CH_4/N_2 molecules from the cage's branch region because they suffer a larger entropic penalty due to the restriction of their rotational motion therein. For both CO_2 + CH_4 and CO_2 + N_2 mixtures, the cage was often occupied by more than one gas molecule. While the storage of two CO_2 molecules in the cage's core

DOI: 10.1021/acs.jpcc.7b01260
J. Phys. Chem. C 2017, 121, 12426−12433

region occurred most frequently, situations in which one CO_2 molecule occupies the core region and one CH_4/N_2 molecule occupies the branch/core region also occurred. The study of the adsorption isotherm for CO_2 + CH_4 mixture suggests that the selectivity of CO_2 over CH_4 decreases slightly as gas partial pressure increases because of the entropic effect.

The cage selectivity revealed by our simulations suggests that the existing porous liquids may be effective for separating CO_2 and N_2 and thus useful in carbon capture applications. However, for separating CO_2 and CH_4, which is needed in applications such as shale gas processing, the performance of the current cage molecule remains to be improved. One possible method is to engineer new cage molecules to further enhance their interactions with the CO_2 molecules without notably enhancing the CH_4−cage interactions. Since CO_2 has a large quadrupole moment while CH_4 has zero quadrupole moment, this may be achieved by introducing functional motifs within the cage that carry significant partial charge. However, such motifs must be approached closely by the CO_2 molecules since charge−quadrupole interactions are short-ranged.

■ ASSOCIATED CONTENT

Supporting Information

The Supporting Information is available free of charge on the ACS Publications website at DOI: 10.1021/acs.jpcc.7b01260.

The density of gas molecules across the simulation box for all systems studied and the density isosurface of CO_2 and N_2 molecules inside the cage molecule when the cage is in equilibrium with gas baths containing pure CO_2, pure N_2, and 1:1 CO_2 + N_2 mixture (PDF)

Trajectory video for the simulation of CO_2 + CH_4 mixture (MPG)

■ AUTHOR INFORMATION

Corresponding Author

*Phone 540-231-7199; e-mail ruiqiao@vt.edu (R.Q.).

ORCID

Jingsong Huang: 0000-0001-8993-2506

Bobby G. Sumpter: 0000-0001-6341-0355

Rui Qiao: 0000-0001-5219-5530

Notes

The authors declare no competing financial interest.

■ ACKNOWLEDGMENTS

We thank the ARC at Virginia Tech for generous allocations of computer time. We also thank the anonymous referees for helpful suggestions. R.Q. was partially supported by an appointment to the HERE program for faculty at the Oak Ridge National Laboratory (ORNL) administered by ORISE. B.G.S. and J.H. acknowledge work done at the Center for Nanophase Materials Sciences, which is a DOE Office of Science User Facility. B.G.S. acknowledges support from the Center for Understanding and Control of Acid Gas-Induced Evolution of Materials for Energy (UNCAGE-ME), an Energy Frontier Research Center funded by the U.S. Department of Energy (DOE), Office of Science, Basic Energy Sciences.

■ REFERENCES

(1) Wright, P. A. *Microporous Framework Solids*; Royal Society of Chemistry: New York, 2008.

(2) Li, H.; Eddaoudi, M.; O'Keeffe, M.; Yaghi, O. M. Design and Synthesis of an Exceptionally Stable and Highly Porous Metal-Organic Framework. *Nature* **1999**, *402*, 276−279.

(3) Szostak, R. *Molecular Sieves: Principles of Synthesis and Identification*; Springer: Cambridge, UK, 1989.

(4) Zhou, H. C.; Long, J. R.; Yaghi, O. M. Introduction to Metal-Organic Frameworks. *Chem. Rev.* **2012**, *112*, 673−674.

(5) Simon, P.; Gogotsi, Y. Materials for Electrochemical Capacitors. *Nat. Mater.* **2008**, *7*, 845−854.

(6) Yamada, M.; Arai, M.; Kurihara, M.; Sakamoto, M.; Miyake, M. Synthesis and Isolation of Cobalt Hexacyanoferrate/Chromate Metal Coordination Nanopolymers Stabilized by Alkylamino Ligand with Metal Elemental Control. *J. Am. Chem. Soc.* **2004**, *126*, 9482−9483.

(7) Devaux, A.; Popovic, Z.; Bossart, O.; De Cola, L.; Kunzmann, A.; Calzaferri, G. Solubilisation of Dye-Loaded Zeolite L Nanocrystals. *Microporous Mesoporous Mater.* **2006**, *90*, 69−72.

(8) Atwood, J. L.; Barbour, L. J.; Jerga, A.; Schottel, B. L. Guest Transport in a Nonporous Organic Solid via Dynamic van der Waals Cooperativity. *Science* **2002**, *298*, 1000−1002.

(9) Tozawa, T.; Jones, J. T. A.; Swamy, S. I.; Jiang, S.; Adams, D. J.; Shakespeare, S.; Clowes, R.; Bradshaw, D.; Hasell, T.; Chong, S. Y.; et al. Porous Organic Cages. *Nat. Mater.* **2009**, *8*, 973−978.

(10) O'Reilly, N.; Giri, N.; James, S. L. Porous Liquids. *Chem. - Eur. J.* **2007**, *13*, 3020−3025.

(11) Melaugh, G.; Giri, N.; Davidson, C. E.; James, S. L.; Del Popolo, M. G. Designing and Understanding Permanent Microporosity in Liquids. *Phys. Chem. Chem. Phys.* **2014**, *16*, 9422−9431.

(12) Giri, N.; Davidson, C. E.; Melaugh, G.; Del Popolo, M. G.; Jones, J. T. A.; Hasell, T.; Cooper, A. I.; Horton, P. N.; Hursthouse, M. B.; James, S. L. Alkylated Organic Cages: From Porous Crystals to Neat Liquids. *Chem. Sci.* **2012**, *3*, 2153−2157.

(13) Giri, N.; Del Popolo, M. G.; Melaugh, G.; Greenaway, R. L.; Ratzke, K.; Koschine, T.; Pison, L.; Gomes, M. F. C.; Cooper, A. I.; James, S. L. Liquids with Permanent Porosity. *Nature* **2015**, *527*, 216−220.

(14) Zhang, J. S.; Chai, S. H.; Qiao, Z. A.; Mahurin, S. M.; Chen, J. H.; Fang, Y. X.; Wan, S.; Nelson, K.; Zhang, P. F.; Dai, S. Porous Liquids: A Promising Class of Media for Gas Separation. *Angew. Chem., Int. Ed.* **2015**, *54*, 932−936.

(15) Holst, J. R.; Trewin, A.; Cooper, A. I. Porous Organic Molecules. *Nat. Chem.* **2010**, *2*, 915−920.

(16) Reiss, P. S.; Little, M. A.; Santolini, V.; Chong, S. Y.; Hasell, T.; Jelfs, K. E.; Briggs, M. E.; Cooper, A. I. Periphery-Functionalized Porous Organic Cages. *Chem. - Eur. J.* **2016**, *22*, 16547−16553.

(17) Hasell, T.; Cooper, A. I. Porous Organic Cages: Soluble, Modular and Molecular Pores. *Nat. Rev. Mater.* **2016**, *1*, 16053.

(18) Mastalerz, M. Liquefied Molecular Holes. *Nature* **2015**, *527*, 174−176.

(19) Hasell, T.; Zhang, H. F.; Cooper, A. I. Solution-Processable Molecular Cage Micropores for Hierarchically Porous Materials. *Adv. Mater.* **2012**, *24*, 5732−5737.

(20) Brutschy, M.; Schneider, M. W.; Mastalerz, M.; Waldvogel, S. R. Porous Organic Cage Compounds as Highly Potent Affinity Materials for Sensing by Quartz Crystal Microbalances. *Adv. Mater.* **2012**, *24*, 6049−6052.

(21) Zhu, G. H.; Hoffman, C. D.; Liu, Y.; Bhattacharyya, S.; Tumuluri, U.; Jue, M. L.; Wu, Z. L.; Sholl, D. S.; Nair, S.; Jones, C. W.; et al. Engineering Porous Organic Cage Crystals with Increased Acid Gas Resistance. *Chem. - Eur. J.* **2016**, *22*, 10743−10747.

(22) Greenaway, R. L.; Holden, D.; Eden, E. G. B.; Stephenson, A.; Yong, C. W.; Bennison, M. J.; Hasell, T.; Briggs, M. E.; James, S. L.; Cooper, A. I. Understanding Gas Capacity, Guest Selectivity, and Diffusion in Porous Liquids. *Chem. Sci.* **2017**, *8*, 2640−2651.

(23) Zhang, F.; Yang, F. C.; Huang, J. S.; Sumpter, B. G.; Qiao, R. Thermodynamics and Kinetics of Gas Storage in Porous Liquids. *J. Phys. Chem. B* **2016**, *120*, 7195−7200.

(24) Goodbody, S. J.; Watanabe, K.; Macgowan, D.; Walton, J. P. R. B.; Quirke, N. Molecular Simulation of Methane and Butane in Silicalite. *J. Chem. Soc., Faraday Trans.* **1991**, *87*, 1951−1958.

(25) Maitland, G. C.; Rigby, M.; Smith, E. B.; Wakeham, W. A. *Intermolecular Forces: Their Origin and Determination*; Clarendon Press: Oxford, UK, 1981.
(26) Katagiri, T.; Takahashi, S.; Tanaka, Y.; Kawabata, K.; Hattori, Y.; Kaneko, K.; Uneyama, K. Gas Storage in Soft 1D Nano-Tunnels by the Induced Fit of a Serration Structure. *CrystEngComm* **2009**, *11*, 347−350.
(27) Jorgensen, W. L.; Maxwell, D. S.; TiradoRives, J. Development and Testing of the OPLS All-Atom Force Field on Conformational Energetics and Properties of Organic Liquids. *J. Am. Chem. Soc.* **1996**, *118*, 11225−11236.
(28) Harris, J. G.; Yung, K. H. Carbon Dioxides Liquid-Vapor Coexistence Curve and Critical Properties as Predicted by a Simple Molecular Model. *J. Phys. Chem.* **1995**, *99*, 12021−12024.
(29) Potoff, J. J.; Siepmann, J. I. Vapor-Liquid Equilibria of Mixtures Containing Alkanes, Carbon Dioxide, and Nitrogen. *AIChE J.* **2001**, *47*, 1676−1682.
(30) Liu, B.; Smit, B. Comparative Molecular Simulation Study of CO_2/N_2 and CH_4/N_2 Separation in Zeolites and Metal-Organic Frameworks. *Langmuir* **2009**, *25*, 5918−5926.
(31) Hess, B.; Kutzner, C.; van der Spoel, D.; Lindahl, E. Gromacs 4: Algorithms for Highly Efficient, Load-Balanced, and Scalable Molecular Simulation. *J. Chem. Theory Comput.* **2008**, *4*, 435−447.
(32) Hess, B.; Bekker, H.; Berendsen, H. J. C.; Fraaije, J. G. E. M. Lincs: A Linear Constraint Solver for Molecular Simulations. *J. Comput. Chem.* **1997**, *18*, 1463−1472.
(33) Martinez, L.; Andrade, R.; Birgin, E. G.; Martinez, J. M. Packmol: A Package for Building Initial Configurations for Molecular Dynamics Simulations. *J. Comput. Chem.* **2009**, *30*, 2157−2164.
(34) Talbot, J. Analysis of Adsorption Selectivity in a One-Dimensional Model System. *AIChE J.* **1997**, *43*, 2471−2478.
(35) Du, Z. M.; Manos, G.; Vlugt, T. J. H.; Smit, B. Molecular Simulation of Adsorption of Short Linear Alkanes and Their Mixtures in Silicalite. *AIChE J.* **1998**, *44*, 1756−1764.

DOI: 10.1021/acs.jpcc.7b01260
J. Phys. Chem. C 2017, 121, 12426−12433